In vivo Optical Coherence Tomography Imaging of Preinvasive Bronchial Lesions

Stephen Lam,[1] Beau Standish,[2] Corisande Baldwin,[1] Annette McWilliams,[1] Jean leRiche,[1] Adi Gazdar,[3] Alex I. Vitkin,[2] Victor Yang,[2] Norihiko Ikeda,[4] and Calum MacAulay[1]

Abstract

Purpose: Optical coherence tomography (OCT) is an optical imaging method that can visualize cellular and extracellular structures at and below tissue surface. The objective of the study was to determine if OCT could characterize preneoplastic changes in the bronchial epithelium identified by autofluorescence bronchoscopy.

Experimental Design: A 1.5-mm fiberoptic probe was inserted via a bronchoscope into the airways of 138 volunteer heavy smokers participating in a chemoprevention trial and 10 patients with lung cancer to evaluate areas that were found to be normal or abnormal on autofluorescence bronchoscopy. Radial scanning of the airways was done to generate OCT images in real time. Following OCT imaging, the same sites were biopsied for pathologic correlation.

Results: A total of 281 OCT images and the corresponding bronchial biopsies were obtained. The histopathology of these areas includes 145 normal/hyperplasia, 61 metaplasia, 39 mild dysplasia, 10 moderate dysplasia, 6 severe dysplasia, 7 carcinoma *in situ*, and 13 invasive carcinomas. Quantitative measurement of the epithelial thickness showed that invasive carcinoma was significantly different than carcinoma *in situ* ($P = 0.004$) and dysplasia was significantly different than metaplasia or hyperplasia ($P = 0.002$). In addition, nuclei of the cells corresponding to histologic results became more discernible in lesions that were moderate dysplasia or worse compared with lower-grade lesions.

Conclusion: Preliminary data suggest that autofluorescence bronchoscopy–guided OCT imaging of bronchial lesions is technically feasible. OCT may be a promising nonbiopsy tool for *in vivo* imaging of preneoplastic bronchial lesions to study their natural history and the effect of chemopreventive intervention.

Lung cancer is the most common cause of cancer death worldwide, with more than 1.3 million people dying of lung cancer annually (1). The 5-year survival rates after the diagnosis of lung cancer has improved only marginally in the last 3 decades (2). Although early detection and chemoprevention is effective in reducing the incidence and mortality of cancer of the breast, there is considerable skepticism in applying the same cancer control strategy in lung cancer. The most common criticism is the uncertain identity of intraepithelial neoplastic (IEN) lesions and the natural history of these lesions.

There are unique challenges in detecting and treating IEN lesions in the lung compared with other organs. The lung is an internal organ consisting of a complex branching system of conducting airways leading to gas exchange units. Lung cancer consists of four major cell types: squamous cell carcinoma, adenocarcinoma, large cell carcinoma, and neuroendocrine tumors (3). They are preferentially located in different parts of the bronchial tree. For example, squamous cell carcinoma and neuroendocrine tumors are more frequently found in the larger central airways compared with adenocarcinoma, which is more frequently found in the small peripheral airways and lung parenchyma. Autofluorescence bronchoscopy is a major advance to improve detection of preinvasive lesions in the central airways by guiding biopsies (4). It has contributed to improved histopathologic classification and molecular profiling of IEN lesions (5–7). It allows rapid scanning of large areas of the bronchial surface for subtle abnormalities that are not visible to white-light examination. However, the improved sensitivity of autofluorescence bronchoscopy to detect preneoplastic lesions is associated with a decrease in specificity compared with white-light examination due to false-positive fluorescence in areas of inflammation or increase in epithelial thickness (4, 8, 9). Because the histology cannot be predicted from the degree of abnormal fluorescence with certainty, a biopsy is needed for

Authors' Affiliations: [1]Cancer Imaging Department, British Columbia Cancer Agency and the University of British Columbia, Vancouver, British Columbia, Canada; [2]Department of Medical Biophysics, Princess Margaret Hospital, University of Toronto, Toronto, Ontario, Canada; [3]University of Texas Southwestern Medical Center, Dallas, Texas; and [4]Department of Thoracic Oncology and Surgery, International University of Health and Welfare, Mita Hospital, Tokyo, Japan

Received 9/20/07; revised 12/10/07; accepted 12/18/07.

Grant support: NIH-National Cancer Institute grants 1PO1-CA96964 and U01CA96109.

The costs of publication of this article were defrayed in part by the payment of page charges. This article must therefore be hereby marked *advertisement* in accordance with 18 U.S.C. Section 1734 solely to indicate this fact.

Requests for reprints: Stephen Lam, Cancer Imaging Department, British Columbia Cancer Agency, 675 West 10 Avenue, Vancouver, British Columbia, Canada V5Z 1L3. Phone: 604-675-8094; Fax: 604-675-8089; E-mail: slam@bccancer.bc.ca.

doi:10.1158/1078-0432.CCR-07-4418

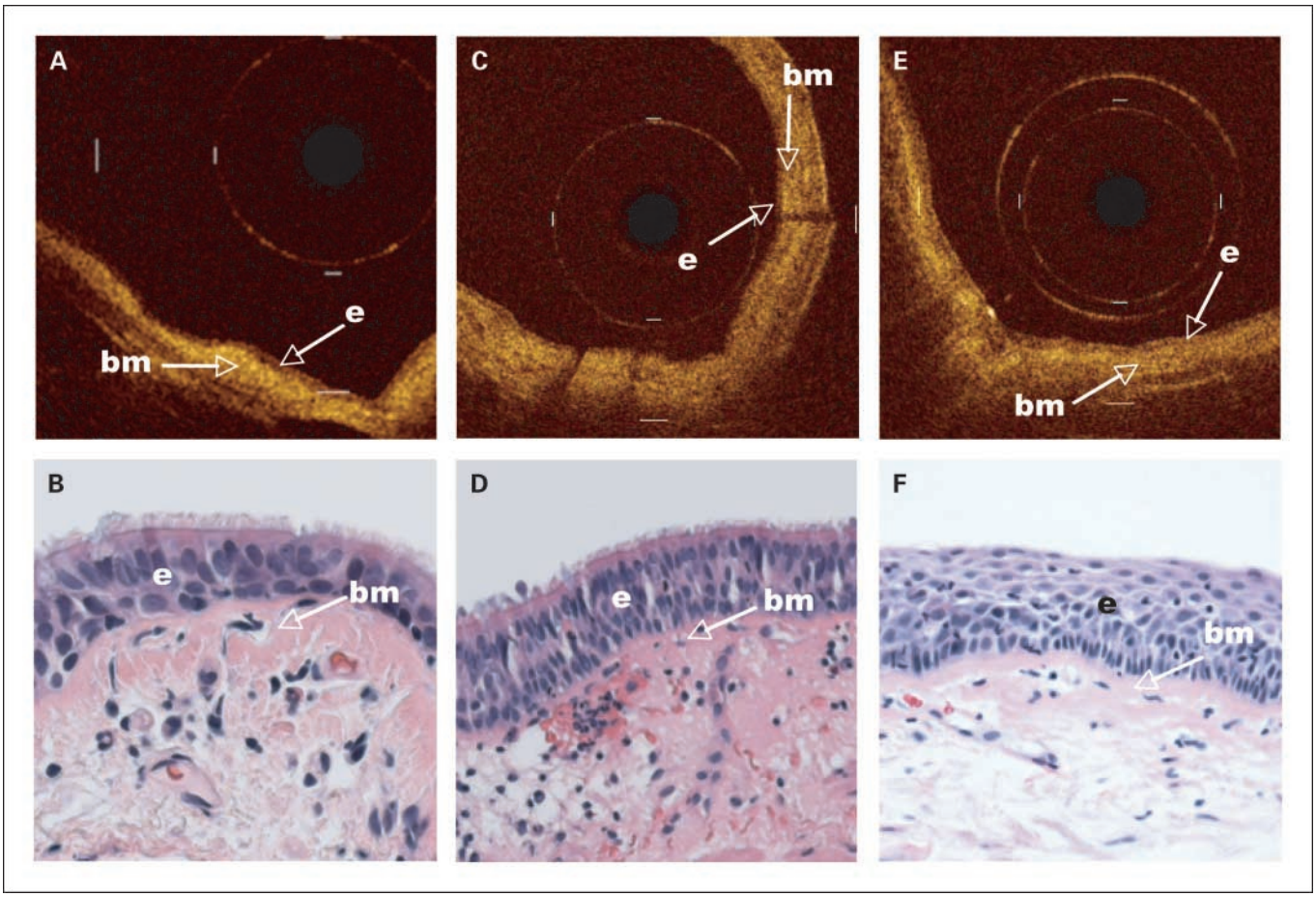

Fig. 1. Representative images of normal healthy human bronchus by standard histologic section (H&E stain; original magnification, ×20; *A*) and OCT (*B*) showing a single-layer epithelium (*e*) on top of the basement membrane (*bm*) and upper submucosa. The basement membrane and upper submucosa are highly reflective due to the presence of collagen. Each calibration mark in the OCT image is equal to 1 mm. *C* and *D,* from an area with hyperplasia. *E* and *F,* from an area with metaplasia.

confirmation. Serial bronchial biopsies are currently used to sample IEN lesions to study the natural history of these lesions and to evaluate the effect of chemopreventive agents in phase II clinical trials (10–15). We have previously reported that 55% of the dysplastic lesions are ≤1.5 mm in size (range, 0.5-1.5 mm; ref. 9). Using careful microdissection and molecular analyses of ~200 cells in contiguous areas of the bronchial epithelium, most of the clonal patches from IEN lesions were found to be very small, containing ~90,000 cells (16). Because the size of a bronchial biopsy forceps is 1.5 mm in diameter, the biopsy procedure itself can potentially remove these lesions mechanically. It is therefore important to develop nonbiopsy methods that can determine the presence and progression/regression of IEN lesions in the bronchial epithelium.

Optical coherence tomography (OCT) is an optical imaging method that can offer microscopic resolution for visualizing cellular and extracellular structures at and below a tissue surface (17–19). In principle, it is similar to ultrasound. Instead of using sound waves, near-IR light is passed into the tissue, and by detecting the reflected light as it interacts with tissue structures as a function of depth, a cross-sectional image is created through optical interferometry. Unlike ultrasound, light waves do not require liquid-based coupling medium and thus are more compatible with airway imaging. There are no associated risks from the weak near-IR light. Preliminary data by one of us (N.I.) suggested that *in situ* and invasive carcinoma can be distinguished from normal bronchial epithelium (20). The intrinsic high spatial resolution of OCT can also become one of its limitations because large amount of data will be accumulated if the entire airway surface is to be imaged at micron-scale resolutions. Autofluorescence bronchoscopy, although lacking the microscopic resolution of OCT, is capable of imaging large portions of the central airway rapidly and may be complementary to OCT.

In the current study, we investigated whether dysplastic lesions and *in situ* carcinoma from high-risk smokers can be distinguished from hyperplasia or metaplasia using OCT. The microscopic OCT imaging is done under the guidance of autofluorescence bronchoscopy. In a large cohort of high-risk heavy smokers, we show for the first time that dysplasia and carcinoma *in situ* (CIS) can be distinguished from lower-grade lesions.

Materials and Methods

Study population and procedures. The study population consisted of participants in two ongoing NIH-National Cancer Institute–sponsored chemoprevention trials (1PO1-CA96964 and U01CA96109). The participants were either current or former smokers ages 45 to 74 y

with a smoking history of ≥30 pack-years. One hundred thirty-eight volunteer smokers, 99 men and 39 women, participated in the study. To determine the differences between CIS and microinvasive/invasive tumors, 10 patients, 7 men and 3 women, undergoing bronchoscopy for diagnosis or treatment of lung cancer were also included into the study. The mean age of the 148 subjects was 62 ± 8 y. Twenty-seven were current smokers and 121 were former smokers. The average smoking intensity was 49 ± 17 pack-years. The study was approved by the Clinical Investigation Committee of the British Columbia Cancer Agency and the University of British Columbia.

White-light and autofluorescence bronchoscopy was done using the Onco-LIFE device (Novadaq Technologies, Inc.) under local anesthesia to the upper airways and conscious sedation as described previously (13–15). Areas suspicious of dysplasia or cancer were noted. Before taking a biopsy, OCT imaging was done by inserting a small optical probe with an outer diameter of 1.5 mm and a depth of focus of 3 mm. The OCT probe was inserted through the biopsy channel of the bronchoscope directly over the site of interest. The OCT image was displayed on a monitor in real time and recorded digitally.

Optical coherence tomography. The OCT system used in the study is a preproduction model, which was developed in a collaboration between LightLab Imaging and Pentax. The design of the system has been described by one of us (N.I.) previously (20). Briefly, low coherence light from a 1,300-nm superluminescent diode source with a bandwidth of 50 nm is split evenly, half toward the bronchial surface via a fiberoptic catheter and half toward a moving mirror. Light is then reflected both from within the tissue and from the mirror. If the distance traveled by light in both arms is nearly identical, interference will occur when the light reflected recombine at the beam splitter. The position of the moving reference arm mirror is precisely controlled electronically. Moving the mirror allows interference (back reflection) information to be obtained from different depths within the sample.

The theoretical axial resolution of the OCT system is 15 to 20 μm. The lateral/transverse resolution is 21 to 27 μm within the appropriate depth of focus (1-2 mm) for bronchial imaging. The position of the focused beam was mechanically scanned across the bronchial luminal surface in 360 degrees at a frame rate of 4 Hz. Axial profiles were digitized for each scan position to create a two-dimensional cross-sectional image.

Correlation of OCT images with pathology of bronchial biopsies. Bronchial biopsies were done in sites with abnormal fluorescence under autofluorescence bronchoscopic guidance as described previously (8, 13–15). Biopsies were also taken from normal control sites as per the chemoprevention trial protocols. The biopsy samples were fixed in buffered formalin, embedded in paraffin, cut into 5 μm sections, and stained with H&E. They were systematically reviewed by two pathologists (J.L. and A.G.) without knowledge of the OCT findings and classified into one of the following eight groups (normal, basal cell hyperplasia, metaplasia, mild/moderate/severe dysplasia, CIS, or invasive carcinoma) according to the WHO criteria (3). Tissue slide examination and micrographs were done with a Nikon Eclipse 80i and recorded with a Nikon digital net camera.

The OCT images were reviewed independently by two scientists (B.S. and S.L.). Normal and abnormal areas were identified. Differences were

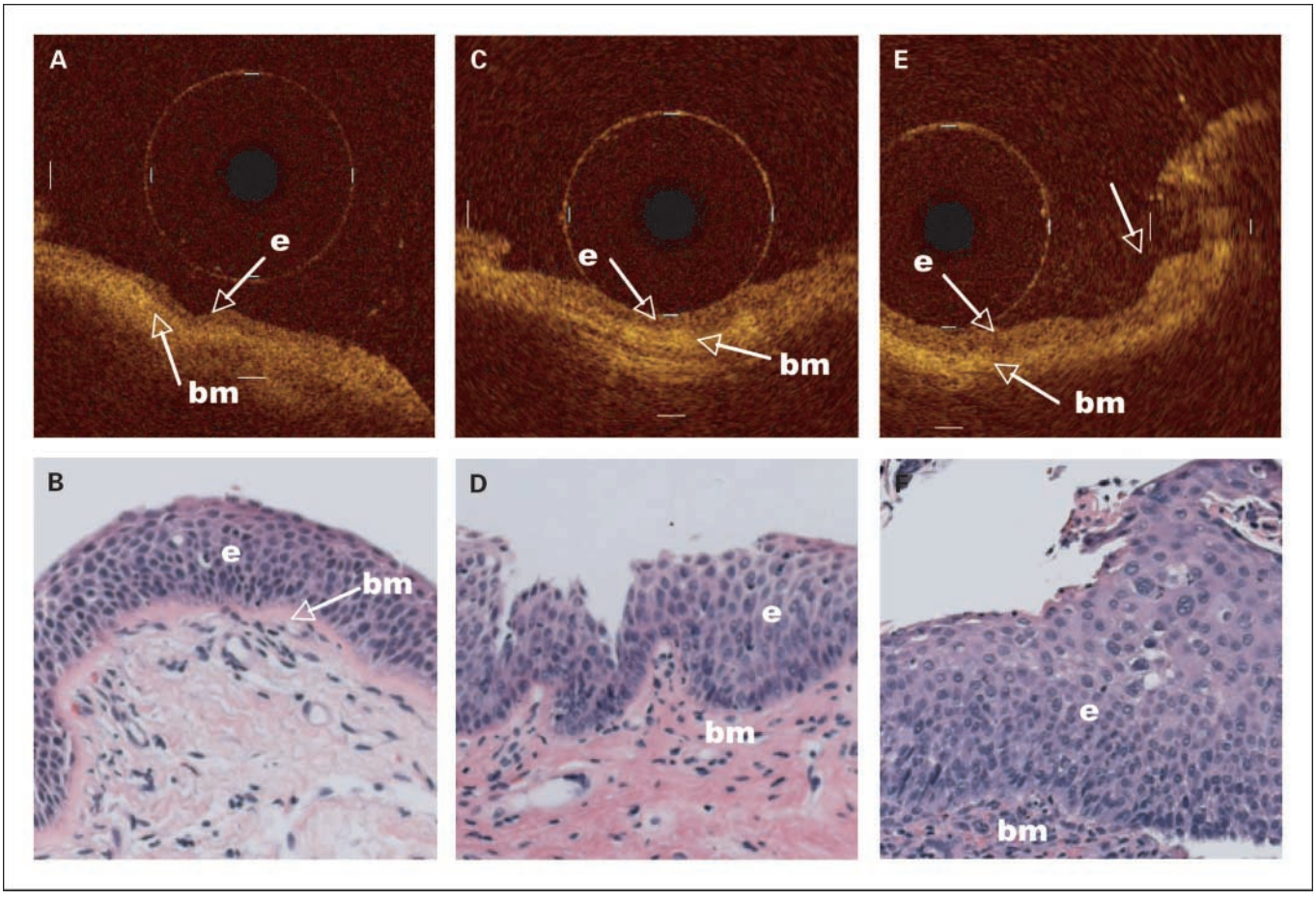

Fig. 2. Representative OCT images of an area with mild dysplasia (*A*), moderate dysplasia (*C*), and severe dysplasia (*E*) and corresponding H&E-stained histologic sections (*B, D*, and *F*; original magnification, ×20). The nuclei in the epithelium become recognizable as darker dots with moderate dysplasia or worse. The arrow in the OCT image of the area with severe dysplasia points to the corresponding elevated area in the H&E section.

resolved by reviewing the images together. The epithelial thickness in the area of interest from the epithelial surface to the basement membrane was quantified by one scientist (B.S.) using ImageJ (Research Services Branch, NIH, Bethesda, MD).

Statistical analysis. The epithelial thickness of the OCT images in different histopathology groups was compared. Normal and hyperplasia were combined into one category for comparison with the higher-grade lesions using the Student's *t* test. All statistical analyses were done using JMP v5.0. All *P* values were two sided and the level of statistical significance was set at $P < 0.05$.

Results

A total of 281 OCT images followed by bronchial biopsy of the same site were taken from the 148 participants. The histopathology of these areas includes 145 normal/hyperplasia, 61 metaplasia, 39 mild dysplasia, 10 moderate dysplasia, 6 severe dysplasia, 7 CIS, and 13 invasive carcinomas. A representative OCT image from each of these seven groups along with the pathology finding is shown in Figs. 1 to 3. Normal or hyperplasia is characterized by one or two cell layers above a highly scattering basement membrane and upper submucosa (Fig. 1). Clear imaging is seen to a depth of ~2 mm to the cartilage layer. As the epithelium changes from normal/hyperplasia to metaplasia, various grades of dysplasia, and CIS, the number of cells in the epithelial layers increases (Figs. 2 and 3). The nuclei became more readily visible in high-grade dysplasia or CIS, although this was at the limit of resolution of the current OCT system. The basement membrane was still intact in CIS (Fig. 3A) but became discontinuous or no longer visible with invasive cancer (Fig. 3C).

The results of the quantitative measurement of the epithelium are shown in Fig. 4. The epithelial thickness was significantly different between invasive cancer and CIS ($P = 0.004$). Severe dysplasia and CIS tended to be thicker than mild or moderate dysplasia but the results did not reach statistical significance ($P = 0.39$). Taken together, mild, moderate, and severe dysplasia were significantly thicker than metaplasia ($P = 0.002$). Mild dysplasia tended to be thicker than metaplasia but the results did not reach statistical significance ($P = 0.069$).

Discussion

The goal of the present study was to establish a library of OCT images with the corresponding pathology finding to determine if OCT can discriminate dysplasia and CIS from normal, hyperplasia, or metaplasia. Our data show that invasive cancer can be distinguished from CIS and that dysplasia can be distinguished from metaplasia, hyperplasia, or normal. Using quantitative measurement, a progressive increase in the epithelial thickness was found to parallel the severity of the histopathology grade. The nuclei of the cells also became more discernible as darker less light scattering objects in lesions that are moderate dysplasia or worse. The basement

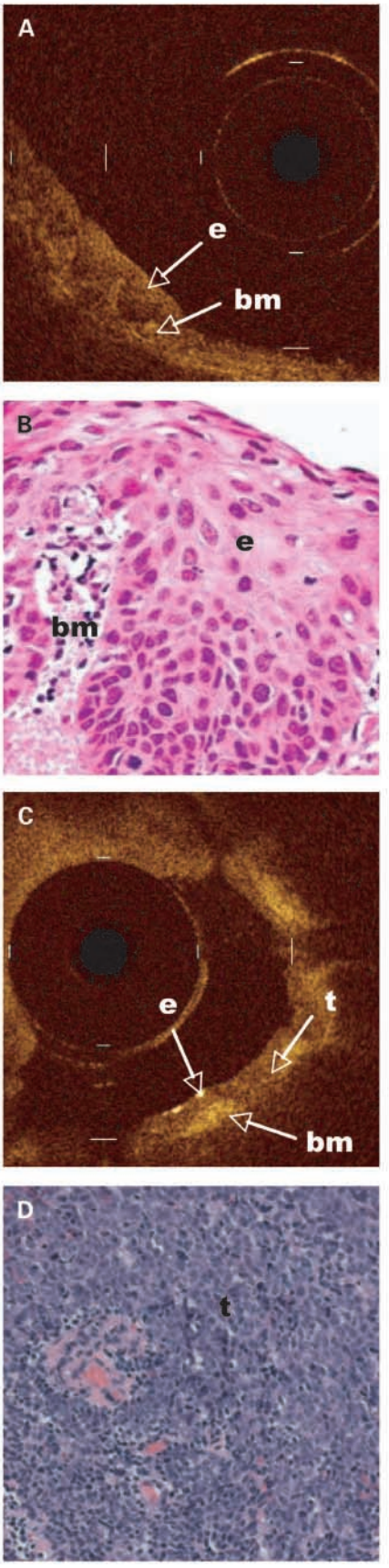

Fig. 3. Representative OCT images of an area with CIS (*A*) and invasive cancer (*C*) and the corresponding H&E-stained histologic section (*B* and *D*; original magnification, ×20). The papillary changes and the enlarged nuclei in the H&E section are clearly recognized in the OCT image as larger, darker, and less scattering dots. For the invasive carcinoma, invasion through the basement membrane in the right lower corner and disappearance of the basement membrane in the upper half of the OCT image can be observed.

membrane became disrupted or disappeared with invasive carcinoma.

There is considerable uncertainty about the natural history of bronchial IEN lesions. Sequential biopsies of the same sites in volunteer smokers with bronchial dysplasia showed a high regression rate at the end of 6 months in those who were in the placebo arm of the chemoprevention trial (13–15). Twenty percent of the current smokers and 50% of the former smokers had complete resolution of their dysplasia to hyperplasia or normal (13–15). Other studies also attempted to clarify the natural history of preneoplastic lesions and CIS using serial bronchoscopy and biopsy (10–12, 21, 22). These studies were relatively small (~50 patients or less). Similar to our shorter-term studies (13–15), >50% of the dysplastic lesions regressed spontaneously on follow-up (8, 10, 11). The extent to which mechanical removal of the dysplastic lesion contributes to the apparently high regression rate of dysplasia is unknown. The high regression rate of bronchial dysplasia complicates the evaluation of chemopreventive agents. A nonbiopsy method would help to clarify the natural history of these lesions and the effect of chemopreventive intervention.

Currently, there are two imaging modalities that have sufficient spatial resolution and tissue depth penetration to study the bronchial epithelial and subepithelial changes associated with lung cancer development. Confocal microendoscopy is an attractive tool as it offers spatial resolution down to the submicron range. However, cells do not emit strong autofluorescence. Although the basement membrane and upper submucosa can be imaged with superb quality, the epithelial cells are not visible (23, 24). In addition, because contact with the bronchial surface is required, the fragile epithelium can be scrapped off during the imaging procedure. Motion artifacts due to cardiac pulsation and respiratory movements can also lead to suboptimal imaging of cellular details. OCT is a noncontact method that delivers near-IR light to the tissue and allows imaging of cellular and extracellular structures from analysis of the back scattered light with a spatial resolution of 4 to 15 μm and a depth penetration of ~2 mm to provide near-histologic images in the bronchial wall (17–20). The fiberoptic probes can be miniaturized to enable imaging of airways down to the terminal bronchiole beyond the range of a standard bronchoscope. The procedure is simple and adds <5 min to a standard bronchoscopic procedure under local anesthesia and conscious sedation. The *in vivo* imaging findings in invasive carcinoma and CIS in the present study are similar to the preliminary study by one of us (N.I.; ref. 20) and the *ex vivo* study by Whiteman et al. (25). We have extended these earlier studies to show that dysplasia (especially high grade) and CIS can be distinguished from lower-grade lesions *in vivo*.

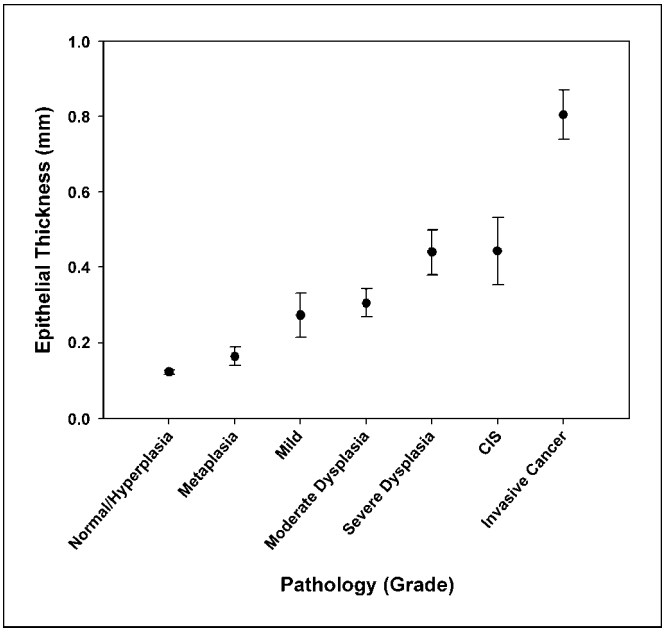

Fig. 4. Quantitative measurements of the epithelium in the OCT images from different histologic grades. There is a progressive increase in the thickness due to a multilayer structure and larger nuclei as the epithelium changes from normal/hyperplasia to metaplasia, mild, moderate, or severe dysplasia, to CIS and invasive carcinoma.

Our study has several important strengths. To our knowledge, this is the first study that combines the large area imaging capability of autofluorescence endoscopy and the microscopic imaging resolution of OCT. Autofluorescence bronchoscopy makes use of fluorescence and absorption properties to provide information about the biochemical composition and metabolic state of bronchial tissues. The fluorescence properties of bronchial tissue are determined by the concentration of the cellular and extracellular fluorophores, their metabolic state, the tissue architecture, and the wavelength-dependent light attenuation due to the concentration as well as distribution of nonfluorescent chromophores such as hemoglobin (3, 26). Collagen and elastin are the most important structural fluorophores. Examples of fluorophores involved in cellular metabolism include NAD^+ and flavins. The autofluorescence yield in the subepithelial tissue is ~10 times higher than the epithelium. As the bronchial epithelium changes from normal to dysplasia, and then to CIS and invasive cancer, there is a progressive decrease in green autofluorescence but proportionately less decrease in red fluorescence intensity. This change is due to a combination of several factors, such as a decrease in the extracellular collagen and elastin, an increase in the number of cell layers associated with dysplasia or cancer, decrease in the fluorescence measured in the bronchial surface due to reabsorption of fluorescent light by a thickened epithelium, increase in absorption of the blue excitation light, and reduced fluorescence due to an increase in the microvascular density/blood volume as well as a reduction in the amount of flavins and NAD^+ in premalignant and malignant cells (3, 26). Because the microvasculature and blood volume is increased in inflammatory lesions and the epithelial thickness is increased with marked goblet cell hyperplasia or metaplasia, false-positive fluorescence can occur in a benign epithelium. Thus, although autofluorescence provides useful information on the biochemical and functional changes in the bronchial epithelium and autofluorescence bronchoscopy serves as a rapid scanning tool to localize preneoplastic and neoplastic lesions, autofluorescence alone cannot be used to study the natural history of these lesions without biopsy confirmation. We systematically examined the changes in the bronchial epithelium associated with the development of squamous cell carcinoma using OCT as a nonbiopsy optical imaging method to provide architectural information in the bronchial epithelium from a large cohort of heavy smokers at risk of developing lung cancer as well as patients with invasive carcinoma. The

multilayer epithelium associated with bronchial dysplasia can be clearly seen. The ability to distinguish dysplasia from lower-grade lesions or inflammation opens the possibility that the effect of chemopreventive agents can be more accurately studied in short-term phase II trials without taking a biopsy before treatment. The same sites can be revisited to document the changes at the end of the treatment period (typically 3-6 months) first by OCT imaging and then by biopsy for histologic confirmation. The spontaneous regression rate of IEN lesions can also be studied in subjects who are treated with placebo. Thus, OCT can complement the rapid scanning ability of autofluorescence bronchoscopy by providing morphologic information to characterize potentially abnormal sites without a biopsy.

Certain limitations to the current study deserve consideration. Different grades of dysplasia could not be distinguished from one another and from CIS using quantitative measurement of the epithelial thickness alone. However, image analysis techniques can be implemented to further investigate the ability of OCT to statistically distinguish different grades of dysplasia from CIS. These techniques include quantifying the SD in OCT signal within a region of interest (27) or texture analysis (28). Architectural measurement of the epithelial changes similar to what has been achieved in morphometric measurements in biopsy specimens (29) may provide an objective grading that is better than the visual grading of the nuclear changes in the present study. Morphometric measurements in OCT images require better spatial resolution than our current OCT device. Systems with higher resolution and Doppler capability that can measure cellular structures in greater detail and quantify vascular density are becoming available for clinical investigation (30, 31). Measurement of second harmonic signal and two-photon excitation coupled with Doppler OCT would further improve the imaging down to the molecular level (32, 33).

In summary, we have shown that autofluorescence endoscopy–guided OCT imaging of bronchial lesions is technically feasible. OCT may be a promising nonbiopsy tool for *in vivo* imaging of preneoplastic bronchial lesions to study their natural history and the effect of chemopreventive agents.

Acknowledgments

We thank Pentax Corp. for providing the OCT device for the study and Myles Mckinnon, Sokhpal Sohi, Edward Mamo, and Sukhinder Khattra for their technical assistance and data management for the study.

References

1. Ezzati M, Lopez AD. Estimates of global mortality attributable to smoking in 2000. Lancet 2003;362:847–52.
2. Jemal A, Siegel R, Ward E, Murray T, Xu J, Thun MJ. Cancer statistics, 2007. CA Cancer J Clin 2007;57:43–66.
3. Travis WD, Colby TV, Corrin B, Shimosato Y, Brambilla E. Histologic and graphical text slides for the histological typing of lung and pleural tumors. In: World Health Organization Pathology Panel: World Health Organization. International classification of tumors. Berlin: Springer Verlag; 1999; p. 5–30.
4. Lam S, McWilliams A. The role of autofluorescence bronchoscopy in diagnosis of early lung cancer. In: Hirsch FR, Bunn Jr PA, Kato H, Mulshine JL, editors. IASLC textbook of prevention and early detection of lung cancer. Taylor and Francis Group UK; 2005; p. 149–60.
5. Wistuba II, Behrens C, Virmani AK, et al. High resolution chromosome 3p allelotyping of human lung cancer and preneoplastic/preinvasive bronchial epithelium reveals multiple, discontinuous sites of 3p allele loss and three regions of frequent breakpoints. Cancer Res 2000;60:1949–60.
6. Garnis C, Davies J, Buys T, et al. Chromosome 5p aberrations and glial cell line-derived neurotrophic factor activation are early events in lung cancer. Oncogene 2005;24:4806–12.
7. Guillaud M, leRiche J, Daw C, et al. Nuclear morphometry as a biomarker for bronchial intraepithelial neoplasia: correlation with genetic damage and cancer development. Cytometry A 2005;63:34–40.
8. Lam S, Kennedy T, Unger M, et al. Localization of bronchial intraepithelial neoplastic lesions by fluorescence bronchoscopy. Chest 1998;113:696–702.
9. Lam S, MacAulay CE, leRiche JC, Palcic B. Detection and localization of early lung cancer by fluorescence bronchoscopy. Cancer 2000;89:2468–73.
10. Breuer RH, Pasic A, Smit EF, et al. The natural course of pre-neoplastic lesions in bronchial epithelium. Clin Cancer Res 2005;15:537–43.
11. Bota S, Auliac JB, Paris C, et al. Follow-up of bronchial precancerous lesions and carcinoma *in situ* using fluorescence endoscopy. Am J Respir Crit Care Med 2001;164:1688–93.
12. Hoshino H, Shibuya K, Chiyo M, et al. Biological features of bronchial squamous dysplasia followed up by autofluorescence bronchoscopy. Lung Cancer 2004;46:187–96.
13. Lam S, MacAulay C, leRiche JC, et al. A randomized phase IIb trial of anethole dithiolethione in smokers with bronchial dysplasia. J Natl Cancer Inst 2002;94:1001–9.
14. Lam S, Xu XC, Parker-Klein H, et al. Surrogate endpoint biomarker analysis in a retinol chemoprevention trial in current and former smokers with bronchial dysplasia. Int J Oncol 2003;23:1607–13.
15. Lam S, leRiche JC, McWilliams A, et al. A randomized phase IIb trial of pulmicort turbuhaler (budesonide) in people with dysplasia of the bronchial epithelium. Clin Cancer Res 2004;10:6502–11.
16. Park IW, Wistuba II, Maitra A, et al. Multiple clonal abnormalities in the bronchial epithelium of patients with lung cancer. J Natl Cancer Inst 1999;91:1863–8.
17. Huang D, Swanson EA, Lin CP, et al. Optical coherence tomography. Science 1991;254:1178–81.
18. Fujimoto JG, Brezinski ME, Tearney GJ, et al. Biomedical imaging and optical biopsy using optical coherence tomography. Nat Med 1995;1:970–2.
19. Tearney GJ, Brezinski ME, Bouma BE, et al. *In vivo* endoscopic optical biopsy with optical coherence tomography. Science 1997;276:2037–9.
20. Tsuboi M, Hayashi A, Ikeda N, et al. Optical coherence tomography in the diagnosis of bronchial lesions. Lung Cancer 2005;49:387–94.
21. Venmans B, van Boxem A, Smit E, Postmus P, Sutedja T. Outcome of bronchial carcinoma *in situ*. Chest 2000;117:1572–6.
22. Weigel TL, Yousem S, Dacic S, Kosco PJ, Siegfried J, Luketich JD. Fluorescence bronchoscopic surveillance after curative surgical resection for non-small-cell lung cancer. Ann Surg Oncol 2000;7:176–80.
23. Thiberville L, Moreno-Swirc S, Vercauteren T, Peltier E, Cave C, Heckly GB. *In vivo* imaging of the bronchial wall microstructure using fibered confocal fluorescence microscopy. Am J Respir Crit Care Med 2007;175:22–31.
24. MacAulay C, Lane P, Richards-Kortum R. *In vivo* pathology: microendoscopy as a new endoscopic imaging modality. In: Van Dam J, editor. Gastrointestinal endoscopy clinics of North America: optical biopsy. Elsevier Netherlands; 2004. p. 595–620.
25. Whiteman SC, Yang Y, van Pittius DG, Stephens M, Parmer J, Spiteri MA. Optical coherence tomography: real-time imaging of bronchial airways microstructure and detection of inflammatory/neoplastic morphological changes. Clin Cancer Res 2006;12:813–8.
26. Wagnieres G, McWilliams A, Lam S. Lung cancer imaging with fluorescence endoscopy. In: Mycek M, Pogue B, editors. Handbook of biomedical fluorescence. New York: Marcel Dekker; 2003. p. 361–96.
27. Tearney GJ, Yabushita H, Houser SL, et al. Quantification of macrophage content in atherosclerotic plaques by optical coherence tomography. Circulation 2003;107:113–9.
28. Qi X, Sivak MV, Isenberg G, Willis JE, Rollins AM. Computer-aided diagnosis of dysplasia in Barrett's esophagus using endoscopic optical coherence tomography. J Biomed Opt 2006;11:044010.
29. Guillaud M, Cox D, Storthz KA, et al. Exploratory analysis of quantitative histopathology of cervical intraepithelial neoplasia: objectivity, reproducibility, malignancy-associated changes, and human papillomavirus. Cytometry A 2004;60:81–9.
30. Yang VXD, Tang S, Gordon ML, et al. Endoscopic Doppler optical coherence tomography in the human GI tract: initial experience. Gastrointest Endosc 2005;61:879–90.
31. Standish BA, Yang VXD, Munce NR, et al. Doppler optical coherence tomography monitoring of microvascular response during photodynamic therapy in a Barrett's esophagus rat model. Gastrointest Endosc 2007;66:326–33.
32. Tang S, Sun CH, Krasieva TB, Chen ZP, Tromberg BJ. Imaging sub-cellular scattering contrast using combined optical coherence and multiphoton microscopy. Opt Lett 2007;32:50305.
33. Tang S, Krasieva TB, Chen ZP, Tromberg BJ. Combined multiphoton microscopy and optical coherence tomography using a 12-fs, broadband source. J Biomed Opt 2006;11:020502.